Kink Bands in a Lamellar Diblock Copolymer Induced by Large Amplitude Oscillatory Shear

ARTICLE *in* MACROMOLECULES · DECEMBER 1996

Impact Factor: 5.8 · DOI: 10.1021/ma960831i

2 AUTHORS, INCLUDING:

Karen I Winey
University of Pennsylvania
331 PUBLICATIONS **11,291** CITATIONS

Kink Bands in a Lamellar Diblock Copolymer Induced by Large Amplitude Oscillatory Shear

Daniel L. Polis and Karen I. Winey*

Laboratory for Research on the Structure of Matter, Department of Materials Science and Engineering, University of Pennsylvania, Philadelphia, Pennsylvania 19104-6272

Received June 7, 1996; Revised Manuscript Received September 17, 1996[⊗]

ABSTRACT: Recent studies have induced a biaxial texture in lamellae-forming poly(styrene-*b*-ethylene propylene) diblock copolymers by applying large amplitude oscillatory shear. According to small-angle X-ray scattering, this biaxial texture consists of "parallel" lamellae (normal to lamellae aligned perpendicular to the shearing surfaces) and "transverse" lamellae (normal to lamellae aligned parallel to the shearing direction). This study determines the arrangement of these two populations of lamellae by using field emission scanning electron microscopy to examine the microstructure and superstructure. The transverse lamellae are separated from the parallel lamellae by sets of parallel wall defects which have two characteristic orientations. This parallel−transverse biaxial morphology shows an astonishing resemblance to that of kink bands. The formation of kink bands suggests that the transverse lamellae could be the result of buckling in the parallel lamellae. Relaxation of the kink band superstructure during quiescent annealing occurs primarily by lamellae tilting, rather than twisting, and produces a variety of defect structures.

Introduction

Controlling the orientation of microphase-separated block copolymer microdomains through the application of strong shear is of technological interest. To this end, many researchers have induced macroscopic alignment of lamellae-forming block copolymers into either the parallel or perpendicular orientation using large amplitude oscillatory shear (LAOS). Until recently the third orthogonal orientation, having the normal of the lamellae parallel to the shearing direction, had not been observed following LAOS. This orientation, known previously as forbidden and now as the transverse orientation, has only been reported in a biaxial texture, which contains lamellae in the parallel and transverse orientations.[1−3] The parallel, perpendicular, and transverse orientations are shown schematically in relation to the shearing direction in Figure 1. To date, parallel−transverse biaxial textures induced by LAOS have only been observed in diblock copolymers with significant mechanical contrast between blocks. Zhang and Wiesner[2] observed a biaxial texture in a poly(styrene-*b*-isoprene) diblock copolymer, whereas Okamoto et al.[1] and Pinheiro et al.[3] observed it in similar poly(styrene-*b*-ethylene propylene) diblock copolymers. In-situ small-angle X-ray scattering (SAXS) studies by Okamoto et al. revealed that the parallel−transverse biaxial orientation reaches a constant morphology after only 15 cycles of shear. Pinheiro et al. observed this biaxial texture via SAXS in a quenched sample following 12 h of LAOS (∼7000 cycles). Both groups found that following the cessation of shear the parallel−transverse biaxial texture disappears during quiescent annealing. These observations suggest that this biaxial texture is stabilized by the shearing process, i.e. a shear-stabilized morphology.

In this work[4] we explore the biaxial texture produced by Pinheiro et al. in an attempt to determine the superstructure of the two populations of lamellae (parallel and transverse) and the relaxation mechanism of the shear-stabilized structure upon quiescent annealing. Using field emission scanning electron microscopy (FE-SEM) and a specially designed sample preparation method, we can accurately determine the orientation of the lamellae relative to the shearing direction, which is difficult using conventional sample preparation and transmission electron microscopy (TEM). Composite micrographs were produced by digitally combining spatially adjacent images which provide information regarding both the microstructure (∼35 nm) and the superstructure (∼10 000 nm) in this biaxial texture. These composite micrographs indicate that the anisotropy of the superstructure in this shear-stabilized biaxial texture resembles kink bands.

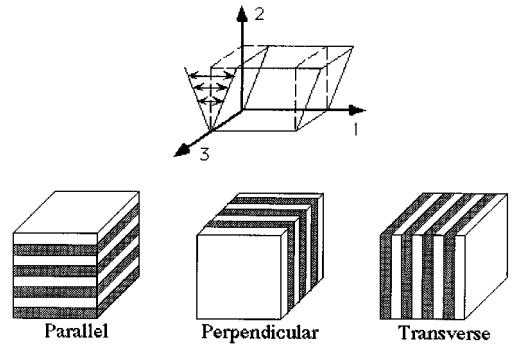

Figure 1. Schematic representation of the parallel, perpendicular, and transverse lamellar orientations relative to the shearing direction. The rheological coordinate system is defined as follows: velocity (1), velocity-gradient (2), and neutral (3) directions.

Experimental Section

Material. The lamellar poly(styrene-*b*-ethylene propylene) diblock copolymer studied was Kraton G1701, provided by Shell Chemical Co. As previously reported, this diblock copolymer has a weight average molecular weight of 110 000 g/mol, a polydispersity index of 1.03, and a styrene monomeric unit content of 37 wt%.[3] The material is therefore referred to as SEP(40−70), corresponding to the nominal average M_w's of the PS and PEP blocks. The microphase separation transition temperature (MST) was not observed upon heating to ∼300 °C and has been estimated to be much greater than 300 °C, making it experimentally inaccessible. The SEP(40−70) samples were produced by solvent casting followed by compression molding.[3]

[⊗] Abstract published in *Advance ACS Abstracts,* November 1, 1996.

S0024-9297(96)00831-5 CCC: $12.00

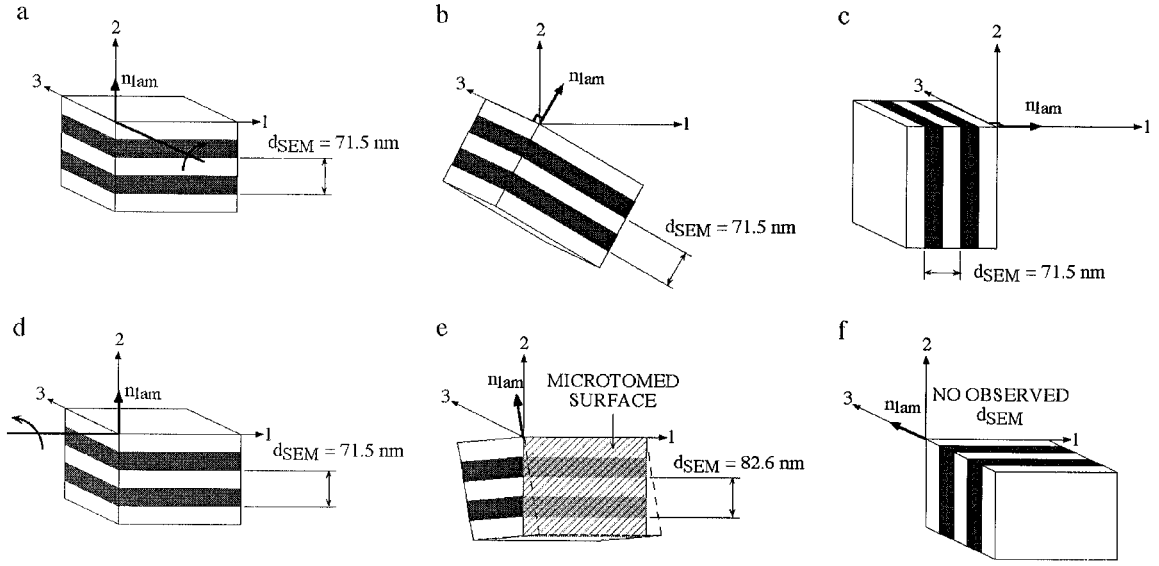

Figure 2. (a−c) Schematic representation of a parallel lamellar grain rotating about the 3 axis (0°, 30°, and 90°) so that the lamellar normal, n_{lam}, remains confined to the 1−2 plane. For these orientations d_{SEM} in the 1−2 image plane remains constant, e.g. $d_{SEM}(a) = d_{SEM}(b) = d_{SEM}(c) = 71.5$ nm. (d−f) Schematic representation of a parallel lamellar grain rotating about the 1 axis (0°, 30°, and 90°). In this rotation n_{lam} rotates out of the 1−2 image plane and thus d_{SEM} varies as a function of the angle between n_{lam} and the 1−2 plane, e.g. $d_{SEM}(d) = 71.5$ nm, $d_{SEM}(e) = 82.6$ nm, and $d_{SEM}(f) = \infty$ (no observed d_{SEM}). Parts a and d correspond to the parallel orientation, c to the transverse orientation, and f to the perpendicular orientation.

Rheology. A Rheometrics Solids Analyzer (RSAII) (oscillatory shear, shear sandwich geometry, 1 mm sample thickness, nitrogen atmosphere) was used to apply LAOS to SEP(40−70). The parallel−transverse biaxial texture was created at a constant strain amplitude, frequency, and temperature of 40%, 1 rad/s, and 150 °C, respectively. This temperature is above the glass transition temperature of the PS block (102 °C) and well below the MST of SEP(40−70). After 12 h of LAOS, samples were quenched (cooled to room temperature in less than 1 min). Specimens for morphological characterization were annealed in a vacuum oven at 150 °C for 2, 48, or 168 h. Note that during the annealing process the 1 mm sample thickness was maintained by confining the specimens to the original mold. Further details of the rheological experiments can be found elsewhere.[3]

FE-SEM. Sample preparation for the FE-SEM was designed to preserve the sample's orientation with respect to the shear field and to provide a large viewing area (~0.1 mm^2). Blocks of approximately 5 mm × 5 mm were cut and mounted on specimen stubs with one of the three orthogonal directions (velocity, gradient, or neutral) oriented perpendicular to the stub surface. The samples were then prepared using a Reichert Ultracut S at −120 °C, which is well below the glass transition temperature of the PEP block. A small mesa, ~0.5 mm × 0.5 mm, was cut on each specimen using a glass knife. A Diatome diamond knife was then used to microtome 70 nm sections from the top of the mesa, thereby removing damage caused by the glass knife and creating a smoother block face. Samples were kept on the microtome stubs during the remainder of the sample preparation and electron microscopy.

Polystyrene latex nanospheres from Polysciences Inc. (Warrington, PA) served as calibrants for the microscope magnification and aided in focusing on the flat samples. These spheres, 503 nm in diameter, were distributed on the samples with an aspirator to prevent them from clustering on the surface. Samples were then stained for 30 min by the vapors of an aqueous solution of 5% RuO_4, which preferentially stains the styrene monomeric units. A coating of Cr, ~4 nm thick, was evaporated onto the samples to reduce charging during scanning electron microscopy.

In order to maximize resolution and minimize charging and sample degradation, the microscopy was performed on a scanning electron microscope equipped with a field emission electron gun (FE-SEM), specifically the JEOL 6300 FV. The FE-SEM was operated at 2 kV. Composite images were made in order to view both the microstructure and superstructure of the lamellae-forming SEP(40−70) samples. Ten to twenty spatially adjacent images were acquired digitally from a sample using JEOL's Vision software. The images were transferred to a Macintosh 7100 where Adobe Photoshop 3.04 was used to create composite micrographs. Typically, 15 μm × 20 μm regions were imaged.

Results

The SAXS results previously reported by Pinheiro et al. are summarized here.[3] Samples of SEP(40−70) subjected to LAOS and quenched exhibit a biaxial texture. This quenched biaxial morphology contains lamellae oriented in the parallel and the nearly transverse directions which have lamellar periods (d_{SAXS}) of 69.0 ± 0.3 nm and 71.5 ± 0.3 nm, respectively. The equilibrium spacing as measured from a cast and quiescently annealed sample is 71.5 ± 0.3 nm. Thus, a 4% thinning of only the parallel lamellae is produced during LAOS. Note that Pinheiro et al. observed the nearly transverse lamellae to be inclined ~80° relative to the parallel lamellae. For the remainder of this paper, we will refer to this nearly transverse orientation as simply transverse. Finally, in situ SAXS revealed that, upon annealing, the parallel lamellae return to the equilibrium spacing, and the transverse lamellae are eliminated.

The nature of this parallel−transverse biaxial texture is most easily discerned from micrographs of the 1−2 plane because the lamellae in both the parallel and transverse orientations are perpendicular to this plane, i.e. the parallel and transverse lamellar normals, $n_{||}$ and n_T, lie within the 1−2 plane; see Figure 1. As we follow the relaxation of this structure, we can differentiate between the rotation of $n_{||}$ and n_T within the 1−2 plane and out of the 1−2 plane using the observed lamellar periods, d_{SEM}. If the parallel or transverse lamellae rotate such that their normals remain in the image plane (1−2 plane), then their corresponding d_{SEM}'s will remain constant throughout the rotation, and moreover $d_{SEM} = d_{SAXS}$. Figure 2a−c shows schematically the effect of rotating a parallel lamellar grain 0° (a), 30° (b), and 90° (c) about the 3 axis; a 90° rotation about the 3

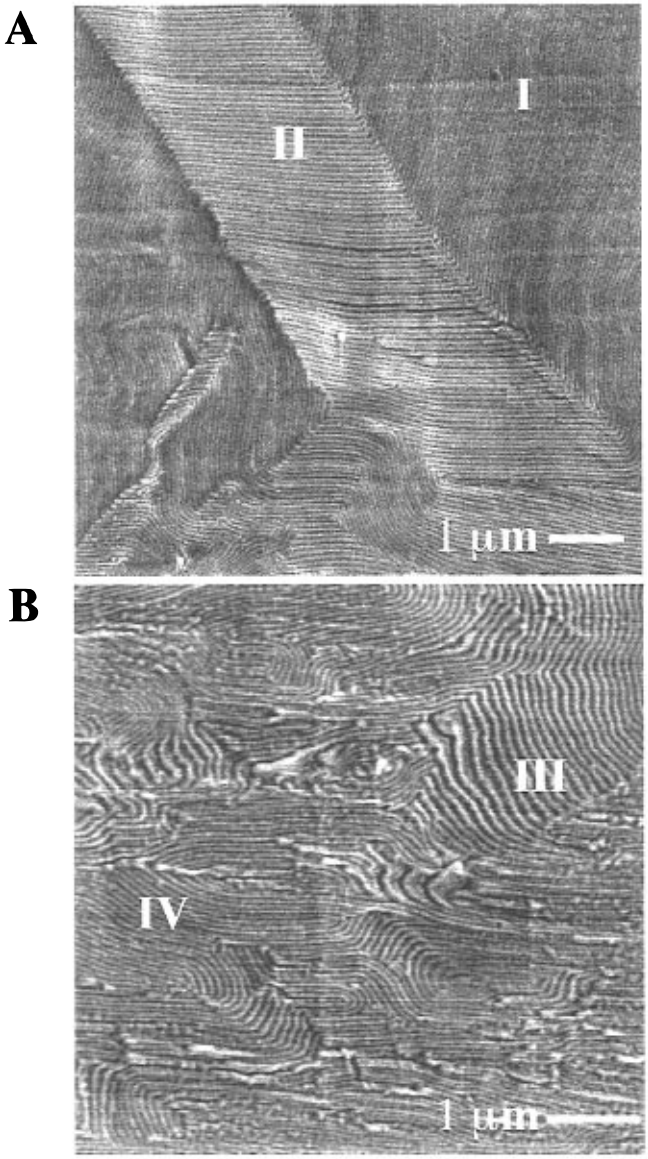

Figure 3. FE-SEM micrographs of SEP(40−70). (a) Two populations of lamellae exist, appearing as vertical (I) or horizontal (II) features. Both populations show a lamellar period equivalent to the equilibrium lamellar period as measured by SAXS ($d_{SEM}(I) \approx d_{SEM}(II) \approx d_{SAXS} \approx 71.5$ nm), suggesting that the lamellar normals are in this image plane. (b) Lamellae exhibit different lamellar periods, $d_{SEM}(III) > d_{SEM}(IV) \approx 71.5$ nm, suggesting that n_{lam} in region III is rotated out of the image plane while n_{lam} in region IV is in the image plane.

axis produces the transverse orientation. In this rotation the normal to the lamellae remains confined to the 1−2 plane producing d_{SEM} (a) = d_{SEM} (b) = d_{SEM} (c) = d_{SAXS}, as observed in images of the 1−2 plane. In contrast, if the lamellar normal (n_{lam}) rotates out of the 1−2 plane, then imaging of the 1−2 plane will produce a $d_{SEM} > d_{SAXS}$. The observed d_{SEM} is a function of the angle between the lamellar normal and the image plane. This is shown schematically in Figure 2d−f: a parallel lamellar grain is rotated 0° (d), 30° (e), and 90° (f) about the 1 axis, which rotates the lamellar normal out of the 1−2 plane. A 90° rotation of this type produces the perpendicular orientation. Images of the 1−2 plane would display a d_{SEM} of 71.5 nm for the 0° rotation, a d_{SEM} of 82.6 nm for the 30° rotation, and no observed d_{SEM} for the 90° rotation, i.e. $d_{SEM}(f) = \infty$.

Figure 3 shows FE-SEM micrographs which display these two situations. Figure 3a contains lamellar

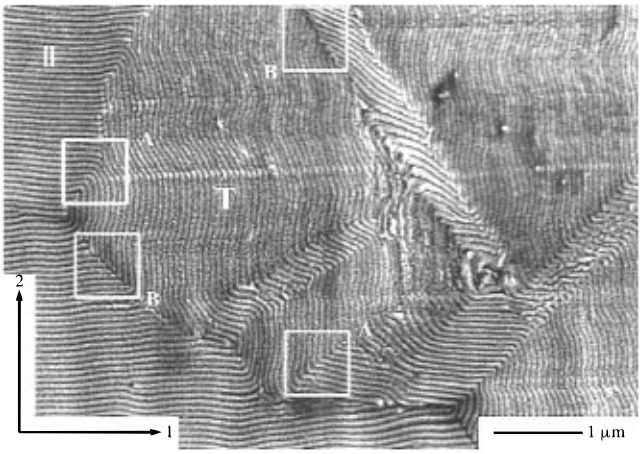

Figure 4. Composite FE-SEM micrograph of SEP(40−70) as-quenched after LAOS showing the microstructure of the oriented lamellae. Regions containing parallel and transverse lamellae are marked with || and T, respectively. Boxes marked A show tilt boundaries in which the lamellae are continuous across the boundary, whereas boxes marked B show T-junction tilt boundaries in which the lamellae are discontinuous across the boundary.

domains with two distinct orientations, I and II. In this micrograph $d_{SEM}(I) \approx d_{SEM}(II) \approx d_{SAXS}$, indicating that both orientations have lamellar normals which lie within this image plane. Figure 3b shows lamellae orientated in a variety of directions, such as III and IV, where $d_{SEM}(III) > d_{SEM}(IV) \approx d_{SAXS}$. We can conclude that the lamellae in region III of Figure 3b have normals rotated out of the image plane, whereas the normals to the lamellae in region IV are in the image plane. While a variation in d_{SEM} for a given sample provides qualitative information regarding the rotation of lamellar domains, precise values of d_{SEM} are unattainable due to slight misorientations during mounting and microtoming.

As previously stated, after the application of LAOS, the as-quenched sample exhibits a parallel−transverse biaxial texture. All the micrographs presented in this paper are of the 1−2 plane because this perspective clearly depicts the parallel and transverse lamellae found in this biaxial texture. A composite micrograph of SEP(40−70) quenched after LAOS is shown in Figure 4. The parallel and transverse lamellae appear as horizontal and vertical features, respectively. The boundary regions between the two populations are narrow; in many places the observed boundary width is smaller than one lamellar long period, i.e. less than 71.5 nm. The majority of boundaries appear to be tilt boundaries, meaning that the normals of the lamellae rotate within the 1−2 plane as the lamellar orientation changes from parallel to transverse. A distinguishing feature of the tilt boundaries is whether or not lamellar continuity is maintained across the boundary. Gido et al. have described in detail three types of tilt boundaries found in lamellar diblocks, two of which have lamellar continuity and will not be differentiated here.[5] Examples of "continuous" tilt boundaries are shown in the boxed regions of Figure 4 marked A. In contrast, T-junction tilt boundaries do not preserve lamellar continuity, as shown in the boxed regions marked B.

The anisotropic shape and arrangement of the regions containing transverse lamellae are apparent in Figure 5, which is a composite FE-SEM micrograph of SEP-(40−70) after LAOS and followed by quenching. The constant d_{SEM} in this 15 × 20 μm image demonstrates that the lamellar normals are confined to the 1−2 plane,

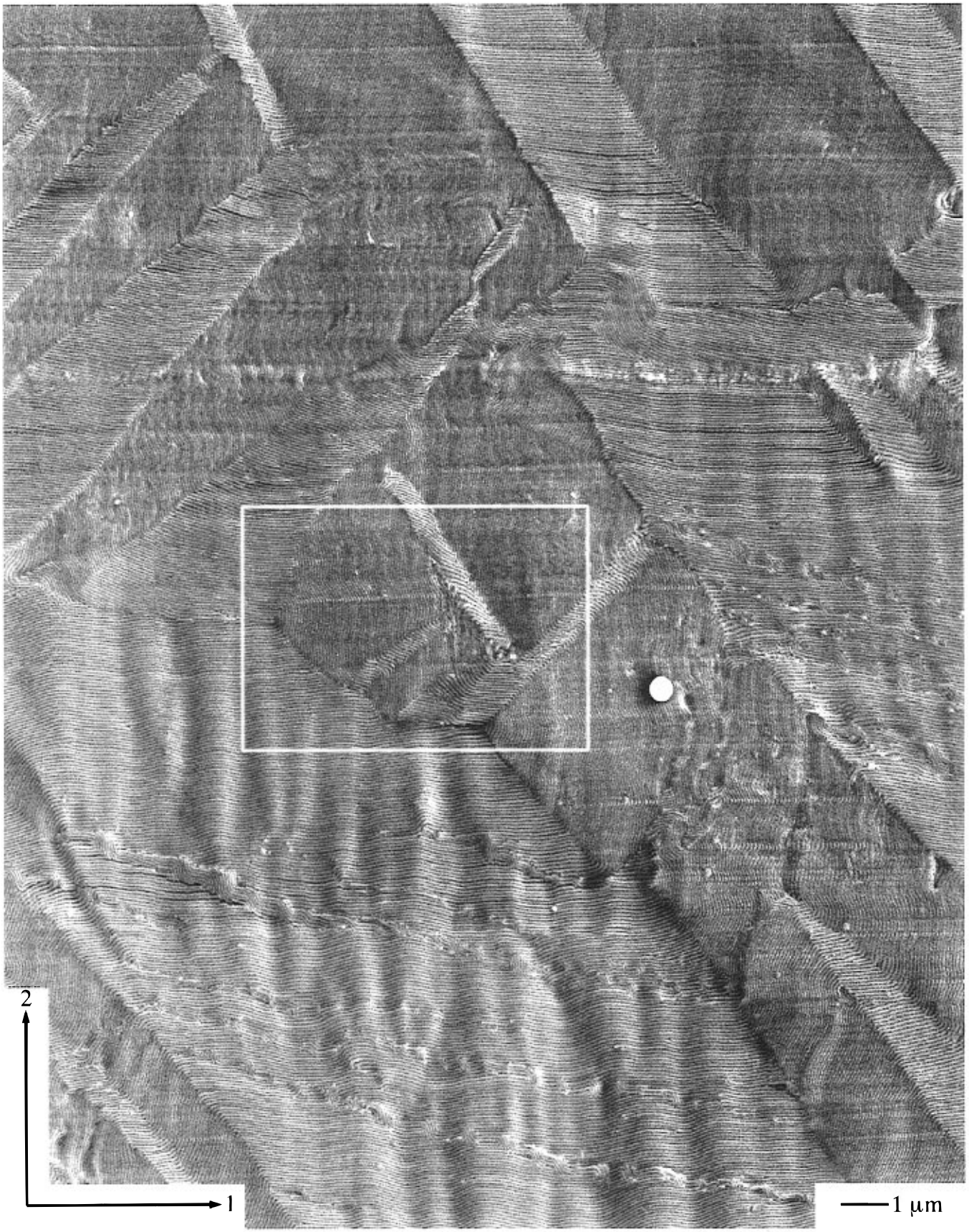

Figure 5. Composite FE-SEM micrograph of SEP(40−70) as-quenched after LAOS showing the superstructure and microstructure of the biaxial texture. The boundaries separating transverse and parallel lamellae are tilt boundaries, containing no twist component. The boxed region is shown at higher magnification in Figure 4.

which further indicates tilt boundaries with no noticeable twist component. It is also evident from this micrograph that the transverse lamellae exist in bands. These bands of transverse lamellae are separated from the parallel lamellae by sets of approximately parallel wall defects or grain boundaries. A modified FE-SEM

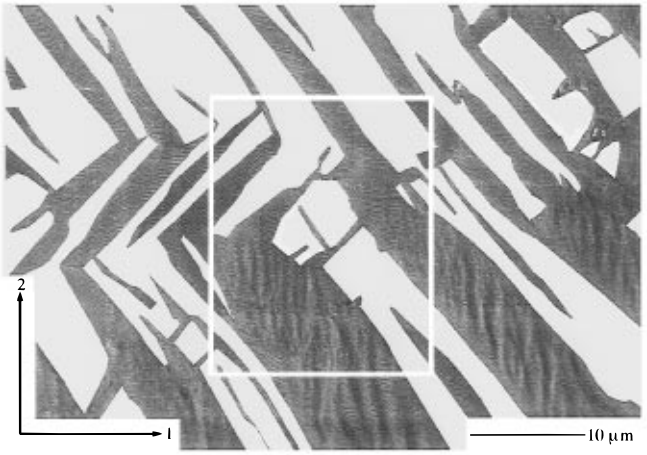

Figure 6. A modified FE-SEM micrograph of SEP(40−70) as-quenched after LAOS showing the superstructure of the parallel−transverse biaxial texture. The large, uniformly light regions are bands containing transverse lamellae, whereas the darker regions contain parallel lamellae. The average boundary orientations are 47° and −49° with respect to the parallel lamellae. The boxed region is shown at higher magnification in Figure 5.

image is shown in Figure 6 to further illustrate this banded superstructure. This FE-SEM micrograph of SEP(40−70) as quenched following LAOS was taken at relatively low magnification, 2000×. Regions of lamellae in the transverse orientation have been colored light gray, while the remaining regions represent domains of parallel lamellae. It is readily evident from this modified FE-SEM image that two sets of bands coexist to form a herringbone pattern. In an effort to quantify the orientation of these bands, straight lines were drawn between the parallel and transverse lamellae to approximate the boundaries. The angles between these boundary lines and the parallel lamellae were measured. Within the field of view of Figure 6, the average boundary orientations of these bands containing transverse lamellae are 47° and −49°, with standard deviations of 3.5° and 5.6°, respectively.

SAXS previously indicated that upon annealing the parallel−transverse biaxial texture in SEP(40−70) becomes primarily parallel, and the parallel lamellae recover to their equilibrium spacing.[3] In an attempt to understand the transformation of the transverse lamellae, we again focus on images taken of the 1−2 plane. Figure 7 is a composite FE-SEM micrograph of SEP(40−70) quenched after LAOS, followed by a 2 h anneal at 150 °C, and then rapidly cooled to room temperature. The relaxation of the parallel−transverse biaxial texture manifests itself as follows. The continuous tilt boundaries widen and the lamellae in the transverse orientation rotate toward the parallel orientation. While the width of the continuous tilt boundaries increases, the few T-junction boundaries remain narrow. Concerning the rotation of the transverse lamellae, the average angle between parallel and transverse lamellae has decreased from ∼82° prior to annealing to ∼74° after a 2 h anneal, as measured from the FFT of 22 μm × 22 μm micrographs. These measurements are consistent with ∼80° and ∼71°, as determined by SAXS, for the as-quenched and 2 h annealed samples, respectively. A constant d_{SEM} in Figure 7 suggests that the initial relaxation has occurred primarily through the rotation of the lamellar normals within the 1−2 plane.

After a 2 h anneal, the macroscopic alignment becomes only slightly perturbed, whereas a 48 h anneal greatly decreases the lamellar alignment, as shown in Figure 8. An in-situ SAXS study indicated that there was still a preferential alignment of the parallel lamellae after a 48 h annealing although a decrease in intensity was observed.[3] The Pinheiro et al. study also revealed an increase in the isotropic scattering in the 1*−2* plane.[3] The boxed regions in Figure 8 show that the lamellae pass through "transition" regions, ∼1 μm in width, between adjacent parallel domains. These transition regions are consistent with a further increase in the tilt boundary width, a corresponding decrease in boundary curvature, and a continued rotation of the initially transverse lamellae toward that of the parallel lamellae. The isotropic scattering is due to both these transition regions as well as an increase of defects other than the wall defects shown in Figure 4. These new defects are characterized by their U shape, as shown in Figure 8. Again, a constant d_{SEM} in this micrograph indicates that this continued relaxation has occurred primarily through the rotation of lamellae during which their normals are confined to the 1−2 plane. These early stages of relaxation imply that one or both of the following may be true: (1) the stored stress produced during extensive LAOS does not posses a twist component; (2) the rotation of lamellar normals out of the 1−2 plane is of considerable energy as compared to the rotation within the 1−2 plane.

Figure 9 shows a composite micrograph corresponding to the 1−2 plane after a 168 h anneal. There are fewer U-shaped defects, but a new defect structure similar to a focal conic structure[6] has become prevalent. The filling of space cannot be accomplished with a true focal conic structure, and thus tilt boundaries are produced which radiate outward from the focal conic.[7] The larger observed period, d_{SEM}, indicates that some of the lamellar normals have rotated out of the 1−2 plane, but the majority of lamellar normals remain in the 1−2 plane. Similar focal conic defects have been observed in other lamellar block copolymers via TEM.[8] This final morphology is certainly unlike the nearly isotropic as-molded initial morphology.

Discussion

Imaging a cryo-ultramicrotomed block face via FE-SEM provides two distinct advantages over the TEM techniques typically used for block copolymer samples. The sample orientation relative to the shear field is maintained throughout the sample preparation following LAOS. Thus the image orientation is known unequivocally during microscopy by simply aligning the edge of the rigid block face and the edge of the field of view. The second advantage with this technique is that large regions can be imaged without interruption by TEM grid bars, section overlap, or section folding. Larger (∼0.25 mm × 0.25 mm), smoother surfaces and composite imaging allow one to obtain information about the microstructure as well as the superstructure, i.e. large, high-resolution images are possible.

Our observations of the parallel−transverse biaxial texture are inconsistent with two possible superstructures. One could hypothesize that either the parallel or the transverse lamellae exist only near the shearing surfaces, while the other orientation is present in the remaining bulk sample. However, microscopy did not reveal any preferential location within the sample for either lamellar orientation. A second possibility is that approximately spherical grains in the initial isotropic sample are unperturbed by the applied shear. It is

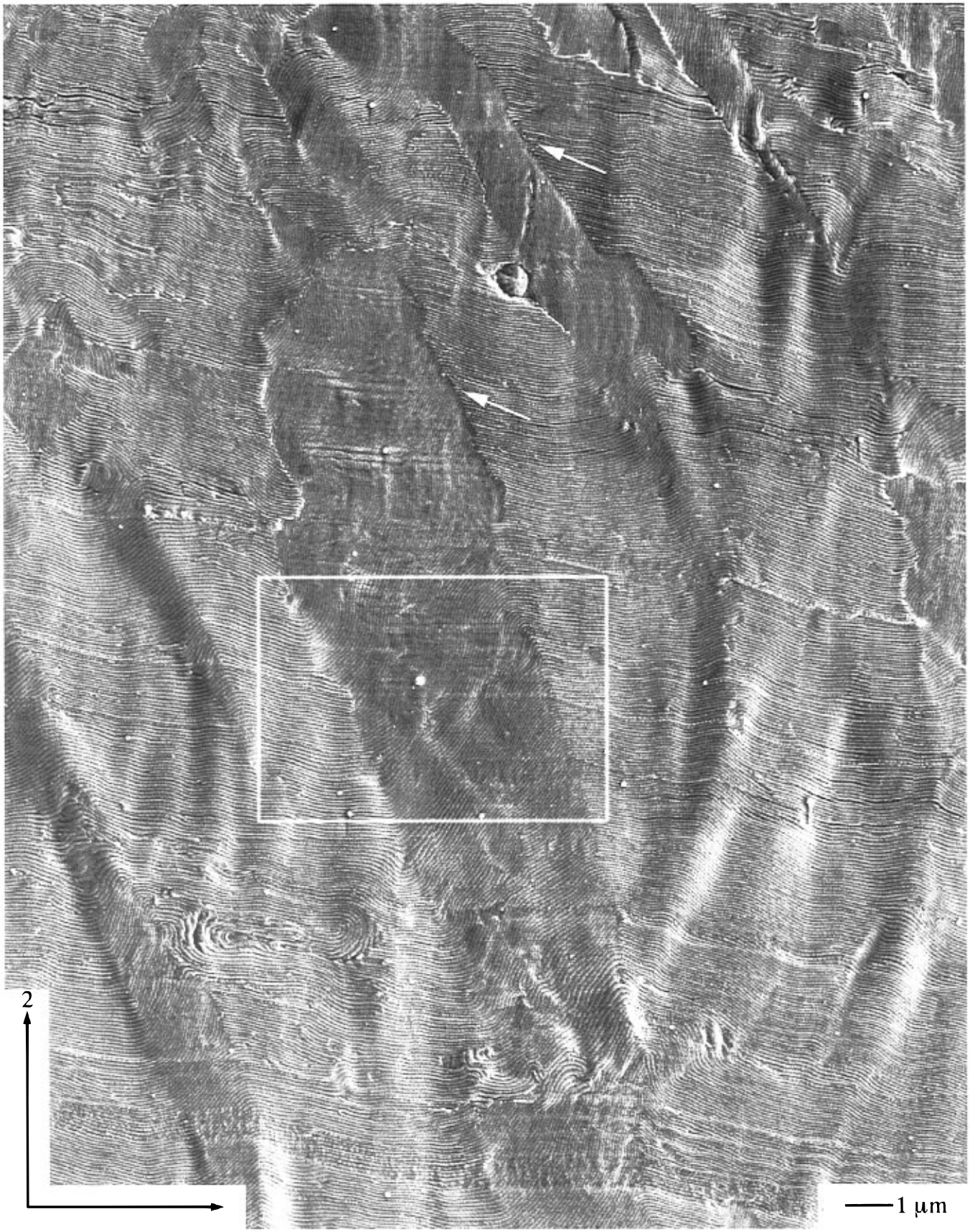

Figure 7. Composite FE-SEM micrograph of SEP(40−70) after LAOS followed by a 2 h anneal at 150 °C. The enclosed transition region shows that (i) the once transverse lamellae are now oriented at a smaller angle relative to the parallel lamellae and (ii) the boundary region has increased in width accompanied by a decreased tilt boundary curvature. T-junction tilt boundaries remain narrow and are denoted by arrows.

evident from Figures 4−6 that this is not the case, because the transverse lamellae exist in well-defined anisotropic bands.

The bands of transverse lamellae which formed in SEP(40−70) during LAOS resemble kink bands. To support this claim characteristics of kink bands are now

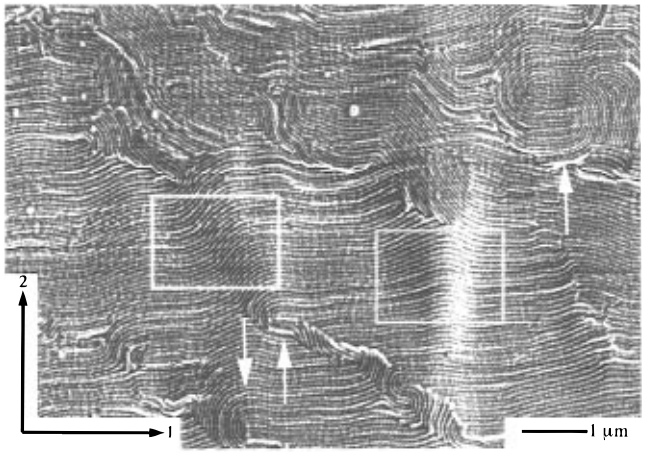

Figure 8. Composite FE-SEM micrograph of SEP(40−70) after LAOS followed by a 48 h anneal at 150 °C. Transition regions, consistent with a further increase in the tilt boundary width, a corresponding decrease in curvature, and a continued rotation of the initially transverse lamellae toward that of the parallel lamellae, are shown in the boxed regions between adjacent parallel domains. A characteristic U-shaped defect has become prevalent, as identified by arrows.

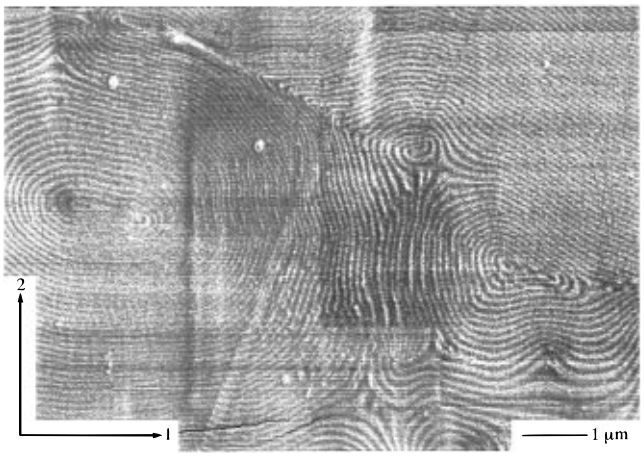

Figure 9. Composite FE-SEM micrograph of SEP(40−70) after LAOS followed by a 168 h anneal at 150 °C. Many of the U-shaped defects have been eliminated. Defect structures similar to focal conic structures appear.

described and compared to the block copolymer system. The material within kink bands is separated from the external material by parallel boundaries, as shown in Figure 10a. This is consistent with the micrograph of SEP(40−70) shown in Figure 5, in which the transverse lamellae are separated from the parallel lamellae by approximately parallel wall defects consisting of tilt boundaries. Furthermore, the growth of kink bands occurs through boundary migration both longitudinally and laterally. Lateral growth via boundary migration is shown schematically between parts a and b of Figure 10. In the case of block copolymers, boundary migration translates into the development of transverse lamellae at the expense of parallel lamellae without the production of intermediate orientations. This growth mechanism is consistent with the micrographs of SEP(40−70) quenched following LAOS, as shown in Figures 4−6, in which primarily parallel and transverse lamellae are observed. In contrast, Figure 10c shows schematically a gradual reorientation between the kink and the external material giving rise to intermediate orientations. While a gradual reorientation process is not consistent with the micrographs of the as-quenched SEP(40−70), this mechanism is similar to the early

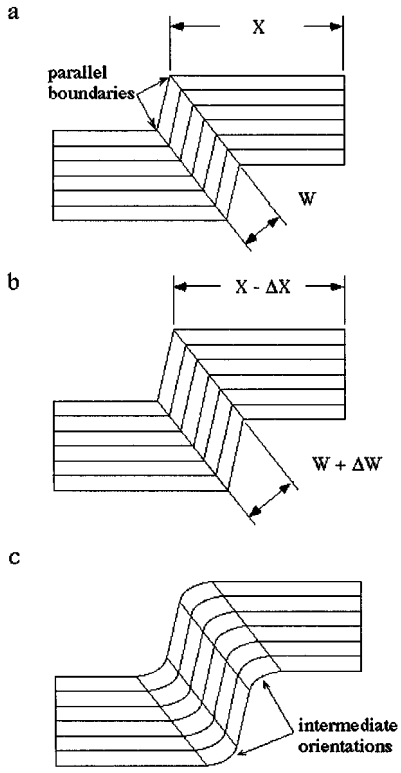

Figure 10. (a) A schematic representation of a kink band. Parallel boundaries separate the external material from the material within the kink band. A schematic showing the growth of a kink band occurring (b) through a boundary migration process and (c) through a gradual reorientation mechanism which produces intermediate layer orientation separating the two primary orientations.

stages of relaxation of the kink bands as shown in Figure 7. Finally, the orientation of kink bands is reported to remain constant during their growth. As of this writing, we have no data to support or refute this characteristic in block copolymer kink bands.

Kink bands have been observed in other layered materials which possess a preferential slip plane. For example, a compressive stress can produce local slip in stacks of rubber sheets[9] or cards,[10] by overcoming the frictional forces between the sheets or cards, to form kink bands. Foliated rocks,[10] such as granite, can preferentially slip between the covalently bonded sheets and also form kink bands. Kink bands have also been observed in nonlayered polymeric materials having a preferred slip direction: oriented crystalline polymers[11] and polymer fibers.[12,13] Lamellae-forming block copolymers with sufficient mechanical contrast between the lamellae, such as SEP(40−70) at 150 °C, have a preferential slip plane. Specifically, the modulus of the PS microdomain is considerably larger than that of the PEP microdomain, so that deformation may occur preferentially in the PEP layer. This characteristic of the block copolymer system appears to be critical in the formation of kink bands.

In conclusion, we hypothesize that the superstructure in SEP(40−70) upon the application of LAOS contains kink bands. If a kinking mechanism is responsible for the parallel−transverse biaxial texture, then the transverse orientation might be the result of buckling of the preferred parallel orientation rather than indicative of an energetically favored orientation. Kinking or buckling would explain why transverse lamellae have only been observed while coexisting with the parallel lamellae.

Acknowledgment. Work at the University of Pennsylvania was supported by NSF-DMR-MRL (9120668), NSF-DMR-YIA (9457997), and Procter & Gamble. D.L.P is grateful for support from a University Fellowship. We acknowledge and thank Dr. Rollin E. Lakis for his advice regarding sample preparation and microscopy techniques and Dr. B. Scott Pinheiro for providing samples.

References and Notes

(1) Okamoto, S.; Saijo, K.; Hashimoto, T. *Macromolecules* **1994**, *27*, 5547.
(2) Zhang, Y.; Wiesner, U. *J. Chem. Phys.* **1995**, *103*, 4784.
(3) Pinheiro, B. S.; Winey, K. I.; Hajduk, D. A.; Gruner, S. M. *Macromolecules* **1996**, *29*, 1482.
(4) Polis, D. L.; Pinheiro, B. S.; Lakis, R. E.; Winey, K. I. In *Microscopy & Microanalysis 1996*; San Francisco Press, Inc.: Minneapolis, MN, 1996; pp 208−209.
(5) Gido, S. P.; Thomas, E. L. *Macromolecules* **1994**, *27*, 6137.
(6) Bouligand, Y. *J. Phys.* **1972**, *33*, 525.
(7) Gido, S. P.; Thomas, E. I. *Macromolecules* **1994**, *27*, 849.
(8) Winey, K. I.; Patel, S. S.; Larson, R. G.; Watanabe, H. *Macromolecules* **1993**, *26*, 2542.
(9) Honea, E.; Johnson, A. M. *Tectonophysics* **1976**, *30*, 197.
(10) Gay, N. C.; Weiss, L. E. *Tectonophysics* **1974**, *21*, 287.
(11) Robertson, R. E. *J. Polym. Sci. Part A-2* **1969**, *7*, 1315.
(12) DeTeresa, S. J.; Porter, R. S.; Farris, R. J. *J. Mater. Sci.* **1988**, *23*, 1886.
(13) Jiang, T.; Rigney, J.; Jones, M. G.; Markoski, L. J.; Spilman, G. E.; Mielewski, D. F.; Martin, D. C. *Macromolecules* **1995**, *28*, 3301.

MA960831I